Parametric identification of the variable structure model of a N_2-laser

L. KAWECKI, T. NIEWIEROWICZ, AND J. DE LA ROSA
Sección de Estudios de Posgrado e Investigación
Escuela Superior de Ingeniería Mecánica y Eléctrica, Instituto Politécnico Nacional
07738 México, D.F., México

Recibido el 3 de junio de 1996; aceptado el 20 de agosto de 1996

ABSTRACT. In this work we propose the analysis of the complete Blumlein circuit for the excitation of a N_2-laser that produces a high order linear integro-differential equations system, when each of the two discharges (the spark gap and the laser chamber) taking place in the circuit are simulated by an inductance and a resistance connected in series. The switching time of both discharges is considered. The solution is found through a parametric identification method based in the measured voltages in the charge capacitors. A Runge-Kutta method for solving the integral terms and a Gauss-Seidel algorithm for the parametric identification were used.

RESUMEN. En este trabajo se propone el análisis del circuito Blumlein completo para la excitación de un láser de N_2, el cual produce un sistema de ecuaciones integro-diferenciales lineales de alto orden, cuando la descarga de interruptor de chispa (spark gap) y de la cámara de descarga láser se representan cada uno por medio de una inductancia y una resistencia conectadas en serie. El tiempo de encendido de cada descarga es considerado en el análisis. La solución se encuentra usando un método de identificación paramétrica basado en los voltajes medidos en los capacitores de carga. Los términos integrales se resuelven usando el método de Runge-Kutta y la identificación paramétrica se hace usando el algoritmo de Gauss-Seidel.

PACS: 42.55

1. INTRODUCTION

For the pulsed excitation of N_2 lasers, two simple electrical circuits are mainly used, known as Blumlein and charge transfer (C-C) circuit. Their role is to produce a very intense uniform glow discharge across the laser head during a very short time. Both circuits (see Fig. 1) consist of two common no-linear elements, a spark gap whose function is to fire the circuit and the laser chamber where the laser discharge takes place. Besides, in order to charge both circuits an impedance Z (it could be a coil or a resistance) parallel to the laser head is used. Traditionally it is supposed that when the spark gap fires the impedance Z shows so high values, in relation to the other elements, that it is possible to eliminate it from the analysis. So, both circuits are reduced to two loops, which follows to a fourth order differential equation for any voltage and current in the circuit, when each discharge taking place in both circuits is simulated by an inductance and a resistance connected in series. The solution of the voltage of these equations is

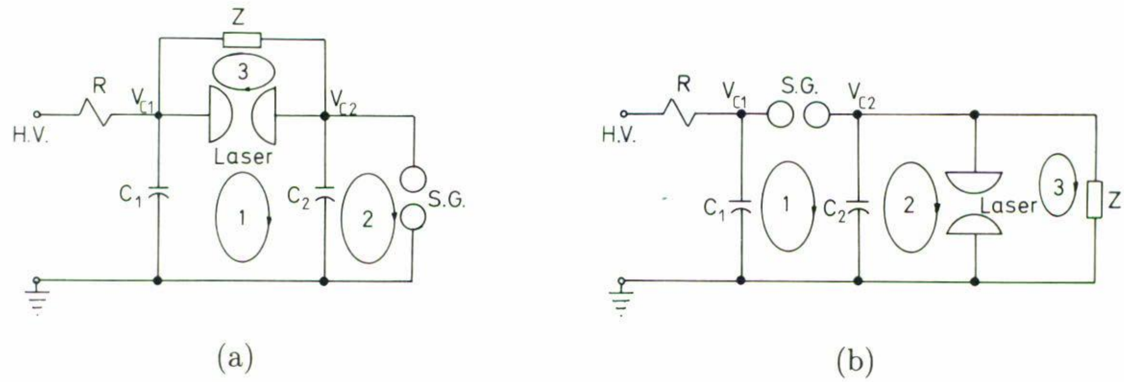

FIGURE 1. Schematic diagram of pulse N_2 lasers. (a) Blumlein circuit. (b) Charge transfer circuit.

given by the following relationship:

$$V(t) = Ae^{-\alpha_1 t}\cos(\omega_1 t) + Be^{-\alpha_2 t}\cos(\omega_2 t + \phi), \tag{1}$$

where the parameters A, B, ω_1, ω_2, α_1, α_2, and ϕ are given by the circuit elements of the equivalent circuit and the initial conditions. Fitting this solution to the experimental laser voltage has been possible [1–5] to find out the parameter values and the average values of the resistances and inductances used to simulate the spark gap and the laser chamber. However, when the obtained parameters are used in the Eq. (1) for the laser voltage a first symmetrical pulse in the wave form is obtained. That is a deviation of the experimental wave form [3], where the leading edge of the pulse is more slowly than the trailing edge.

In this work we propose the analysis of the complete Blumlein circuit considering Z. That produces higher order linear differential equations that can not be solved with the use of Eq. (1). The integro-differential equations of the system are solved through parametric identification method based in the measured voltages in the capacitors C_1 and C_2. A Runge-Kutta method for solving the integral terms and a Gauss-Seidel algorithm for the parametric identification were used. A much better fitting between theoretical and experimental laser voltage is obtained.

2. THEORETICAL CONSIDERATIONS

Figure 1a shows a schematic diagram of the Blumlein circuit. The circuit is composed of a spark gap (S.G.), the laser head, two capacitors and a coil L as the Z impedance. When high voltage is applied, both capacitors are equally charged until the breakdown voltage across S.G. is reached. At this potential, the S.G. fires and C_2 begins to discharge very fast through S.G., so does C_1 but through L and S.G. in a slower way. A very fast rising high voltage difference appears across the laser head until the laser beakdown voltage is reached and the discharge takes place. Figure 2 shows the voltages V_{C_1}, V_{C_2}, and $V_{C_1} - V_{C_2}$. The mechanical construction of the laser is reported elsewhere [6].

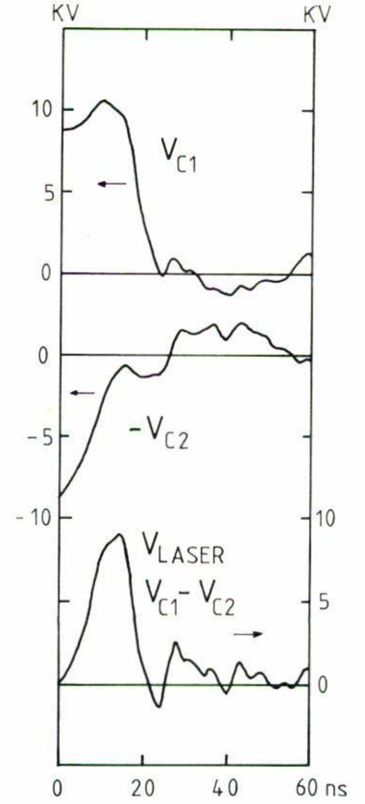

FIGURE 2. From top to bottom: voltage appearing in C_1 (V_{C_1}); voltage in C_2 (V_{C_2}); voltage waveform across the laser head ($V_{C_1} - V_{C_2}$).

The voltages V_{C_1} and V_{C_2} were measured with two equal high voltages probes (Tektronix P6015, rise-time < 4.5 ns) combined with a 300 MHz bandwidth oscilloscope (Tektronix 2440). The voltage in the laser head (Fig. 2) is the voltage difference $V_{C_1} - V_{C_2}$, which was automatically given by the oscilloscope and is the average of 16 discharges. Stable operation of the laser was achieved at voltages ranging from 6 to 12 KV, pressures between 60 and 130 hPa and frequencies up to 20 Hz. The pulse-to-pulse fluctuations of the laser head voltage were less than 5%.

To analyze the circuit, each discharge taking place in the circuit is simulated by an inductance and a resistance connected in series (see Fig. 3). R_1 and L_1 stand for the inductance and a resistance associated with the laser head loop, respectively, and R_2 and L_2 stand for the analogous parameters of the spark gap loop. The differential equation governing the performance of the circuit are given as follows.

2.1. THE FIRST STEP ($0 \leq t \leq t_B$)

At $t = 0$ the S.G. fires and at $t = t_B$ the laser head fires. Through this step, the equivalent circuit showing the operation of the system is shown in Fig. 4a. The equations governing its performance are given as follows:

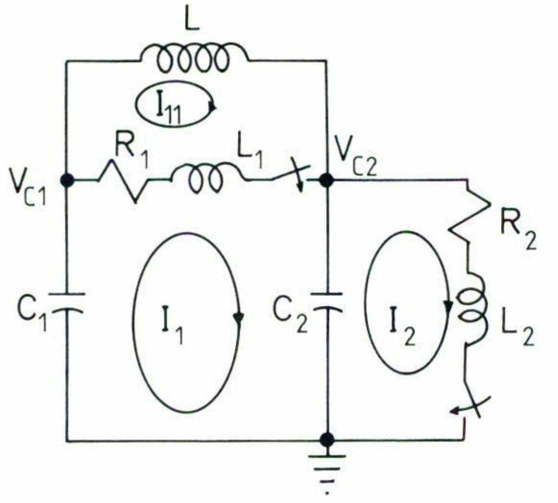

FIGURE 3. Equivalent circuit of the Blumlein circuit.

$$R_2 I_2 + L_2 \frac{dI_2}{dt} + \frac{1}{C_2} \int_0^{t_{\rm B}} (I_2 - I_{11})\, dt + V_{C_2}\big|_{t=0} = 0, \tag{2}$$

$$L \frac{dI_{11}}{dt} + \frac{1}{C_1} \int_0^{t_{\rm B}} I_{11}\, dt + \frac{1}{C_2} \int_0^{t_{\rm B}} (I_{11} - I_2)\, dt + V_{C_1}\big|_{t=0} + V_{C_2}\big|_{t=0} = 0, \tag{3}$$

where

$$V_{C_1}\big|_{t=0} = V_{C_2}\big|_{t=0} = V_H; \tag{4}$$

I_2 and I_{11} can be calculated through a Runge Kutta method. The evaluation of $t_{\rm B}$ could be done from the relation

$$V_{\rm B} = (V_{C_1} - V_{C_2})\big|_{t=t_{\rm B}} = \frac{1}{C_1} \int_0^{t_{\rm B}} I_{11}\, dt + V_{C_1}\big|_{t=0} - \frac{1}{C_2} \int_0^{t_{\rm B}} (I_2 - I_{11})\, dt - V_{C_2}\big|_{t=0}, \tag{5}$$

where $V_{\rm B}$ is obtained from the experimental voltage, *i.e.*,

$$t_{\rm B} = \left\{ t \in [0, t_{\rm FIN}] \colon \frac{1}{C_1} \int_0^{t} I_{11}\, dt + V_{C_1}\big|_{t=0} - \frac{1}{C_2} \int_0^{t} (I_2 - I_{11})\, dt - V_{C_2}\big|_{t=0} = V_{\rm B} \right\}. \tag{6}$$

2.2. THE SECOND STEP ($t_{\rm B} \le t \le t_{\rm FIN}$)

At $t_{\rm FIN}$ the glow discharge in the laser head gets in the break down. Through this step the equivalent circuit showing the operation of the system is shown in Fig. 4b. The equations governing its performance are given as follows:

$$R_1 I_1 + L_1 \frac{dI_1}{dt} + \frac{1}{C_1} \int_{t_{\rm B}}^{t_{\rm FIN}} (I_1 + I_{11})\, dt + V_{C_1}\big|_{t=t_{\rm B}} + \frac{1}{C_2} \int_{t_{\rm B}}^{t_{\rm FIN}} (I_1 + I_{11} - I_2)\, dt + V_{C_2}\big|_{t=t_{\rm B}} = 0, \tag{7}$$

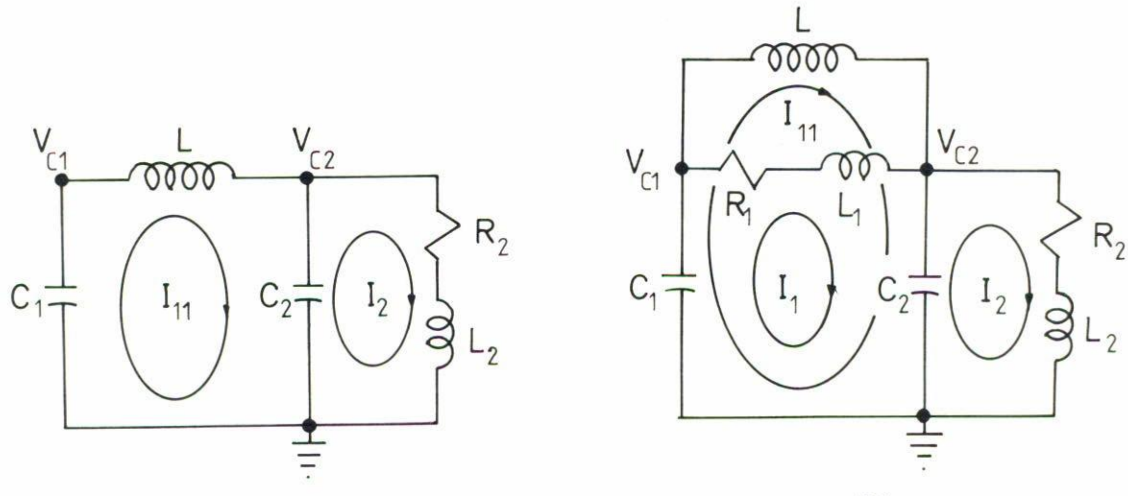

FIGURE 4. Equivalent circuit for the different operation steps of the Blumlein circuit. (a) $0 \leq t \leq t_{\mathrm{B}}$. (b) $t_{\mathrm{B}} \leq t \leq t_{\mathrm{FIN}}$.

$$L\frac{dI_{11}}{dt} + \frac{1}{C_1}\int_{t_{\mathrm{B}}}^{t_{\mathrm{FIN}}} (I_1 + I_{11})\,dt + V_{C_1}\big|_{t=t_{\mathrm{B}}} + \frac{1}{C_2}\int_{t_{\mathrm{B}}}^{t_{\mathrm{FIN}}} (I_1 + I_{11} - I_2)\,dt + V_{C_2}\big|_{t=t_{\mathrm{B}}} = 0, \tag{8}$$

$$R_2 I_2 + L_2\frac{dI_2}{dt} + \frac{1}{C_2}\int_{t_{\mathrm{B}}}^{t_{\mathrm{FIN}}} (I_2 - I_1 - I_{11})\,dt + V_{C_2}\big|_{t=t_{\mathrm{B}}} = 0, \tag{9}$$

where

$$V_{C_1}\big|_{t=t_{\mathrm{B}}} = \frac{1}{C_1}\int_0^{t_{\mathrm{B}}} I_{11}\,dt + V_{C_1}\big|_{t=0}, \tag{10}$$

$$V_{C_2}\big|_{t=t_{\mathrm{B}}} = \frac{1}{C_2}\int_0^{t_{\mathrm{B}}} (I_2 - I_{11})\,dt + V_{C_2}\big|_{t=0}. \tag{11}$$

3. PARAMETRIC IDENTIFICATION

The parametric identification is accomplished through a comparison of the values in the real process and the theoretical model. To do that is necessary to consider n experimental voltage values $V^*_{C_1}(t_k)$ for $k = 1, 2, \ldots, n$, and n experimental voltage values $V^*_{C_2}(t_k)$ for $k = 1, 2, \ldots, n$, satisfying Eqs. (2)–(11).

As parameter identification index we propose

$$J = \sum_{k=1}^{n}\left[\left(V_{C_1}(t_k) - V^*_{C_1}(t_k)\right)^2 + \left(V_{C_2}(t_k) - V^*_{C_2}(t_k)\right)^2\right]. \tag{12}$$

To use Eq. (12) we need the values of R_1, R_2, L_1, L_2, L, C_1, C_2. The last ones are established by design, but R_1, R_2, L_1, L_2, are the non-measurable, non linear resistance and inductance of the laser and spark gap, respectively. Here we consider them as constants. So, we are looking for the values of R_1, R_2, L_1, L_2 for which Eq. (12) has a minimum.

So that the problem is reduced to the minimization

$$\min_{R_1, R_2, L_1, L_2} \sum_{k=1}^{n} \left[\left(V_{C_1}(t_k) - V_{C_1}^*(t_k) \right)^2 + \left(V_{C_2}(t_k) - V_{C_2}^*(t_k) \right)^2 \right]. \tag{13}$$

For $0 \leq t_k \leq t_{\mathrm{B}}, V_{C_1}$ and V_{C_2} are given as follows:

$$V_{C_1}(t_k)\big|_{0 \leq t_k \leq t_{\mathrm{B}}} = \frac{1}{C_1} \int_0^{t_k} I_{11}\, dt + V_{C_1}\big|_{t_k=0}, \tag{14}$$

$$V_{C_2}(t_k)\big|_{0 \leq t_k \leq t_{\mathrm{B}}} = \frac{1}{C_1} \int_0^{t_k} (I_2 - I_{11})\, dt + V_{C_2}\big|_{t_k=0}, \tag{15}$$

where I_2 and I_{11} are calculated from (2) and (3), and for $t_{\mathrm{B}} \leq t_k \leq t_{\mathrm{FIN}}$,

$$V_{C_2}(t_k)\big|_{t_{\mathrm{B}} \leq t_k \leq t_{\mathrm{FIN}}} = \frac{1}{C_2} \int_{t_{\mathrm{B}}}^{t_k} (I_2 - I_1 - I_{11})\, dt + V_{C_2}\big|_{t_k=t_{\mathrm{B}}}, \tag{16}$$

$$V_{C_1}(t_k)\big|_{t_{\mathrm{B}} \leq t_k \leq t_{\mathrm{FIN}}} = \frac{1}{C_1} \int_{t_{\mathrm{B}}}^{t_k} (I_1 + I_{11})\, dt + V_{C_1}\big|_{t_k=t_{\mathrm{B}}}, \tag{17}$$

where I_1, I_{11} and I_2 are calculated from Eqs. (7), (8) and (9).

4. PROPOSED ALGORITHM

The algorithm based on the Gauss-Seidel method used in this work is reported elsewhere [3], and the integrals terms in the equation system are solved using a conventional Runge-Kutta method. The algorithm was written in Fortran v. 5 from Microsoft and a PC Pentium 100 Mhz was used. The solution took approximately 5 hours. To obtain a graphical representation of the voltage we have used an additional Fortran program and the Harvard Graphics software.

5. RESULTS AND CONCLUSIONS

From the experimental voltages V_{C_1} and V_{C_2} (see Fig. 2), we chose 26 values $V_{C_1}^*$ and $V_{C_2}^*$ for calculation (see Table I). After processing with $V_{C_1}(t_k)$ and $V_{C_2}(t_k)$, for $k = 1, 2, \ldots, 26$, we obtained the parameter values shown in Table II.

In Table II the obtained values when the spark gap and the laser head fired at the same time [3] are shown too. In the present model we have that for the laser head $R_1 = \infty$ for $0 \leq t \leq t_{\mathrm{B}}$ (because in this period of time no current flows through the laser head) and $R_1 = 1.644\,\Omega$ and $L_1 = 5.072$ nH for $t_{\mathrm{B}} \leq t \leq t_{\mathrm{FIN}}$, while in our previous

TABLE I. Measured values.

k	$t_k \times 10^{-9}$ [seg]	$V^*_{C_1}(t_k)$ [V]	$V^*_{C_2}(t_k)$ [V]
1	0.0	8857	8857
2	2.22	8857	8286
3	4.44	8611	6944
4	6.66	9428	6000
5	8.88	10 000	4444
6	11.10	10 571	3143
7	13.32	10 000	1389
8	15.54	9714	571
9	17.76	5833	833
10	19.98	4286	1143
11	22.20	1389	1389
12	24.42	0	1389
13	26.64	833	556
14	28.86	833	−833
15	31.08	0	−1389
16	33.30	0	−1143
17	35.52	−1111	−1389
18	37.74	−833	−1571
19	39.96	−1389	−833
20	42.18	−1111	−1389
21	44.40	−833	−1944
22	46.62	−833	−1389
23	48.84	−833	−1111
24	51.06	−417	−833
25	53.28	−556	−556
26	55.50	−571	0

report [3] $R_1 = 3.068\,\Omega$ and $L_1 = 19.09$ nH for $0 \leq t \leq t_{\text{FIN}}$. We conclude that the lower values of R_1 and L_1 calculated in this work, occur because we are considering now that the change of their maximal to their minimal values take place in a shorter time. The two steps model produce a very important change in the value of L_2 and in the relation L_1/L_2. Now the calculated inductance of the laser head is lower than the inductance of the spark gap. This is physically very reasonable because the channel of the discharge in the laser is thicker than the channel of the discharge in the spark gap.

Finally, Fig. 5 shows the voltage behavior obtained with the parameters from Table II and Eqs. (2)–(10). The evolution in the voltages until the first 26 ns, Figs. 2 and 5, show a

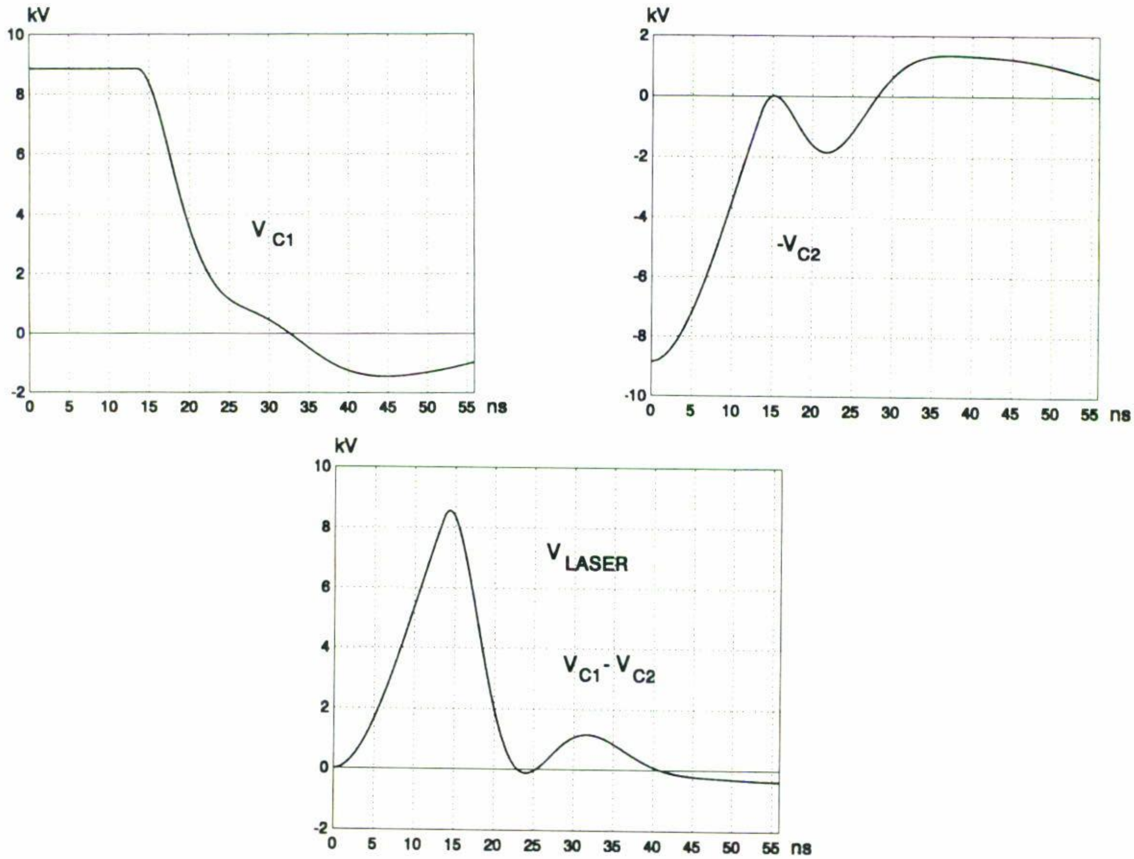

FIGURE 5. Top left: simulated voltage V_{C_1}; top right: voltage V_{C_2}; bottom: voltage across the laser head ($V_{C_1} - V_{C_2}$).

TABLE II. Results of parametric identification.

	This work	From Ref. 3
R_1	1.644 [Ω]	3.068 [Ω]
R_2	1.1936 [Ω]	1.43 [Ω]
L_1	5.072 [nH]	19.09 [nH]
L_2	20.062 [nH]	8.65 [nH]

good fit taking into consideration that a linear mathematical model was used to simulate a nonlinear process. The breakdown in the laser head takes place when $V_{C_1} - V_{C_2}$ reaches its maximum value. From this time on, the process is represented by the equivalent circuit of Fig. 4b, but after laser emission the laser discharge changes into an arc discharge, changing their inductance and resistance drastically. Because this discharge period of time is not interesting for laser emission it has not been analyzed.

While conventional methods of solving Blumlein or charge transfer circuits, like the method used in our previous report [3], do not consider the inductance L and the fire times of the spark gap and the laser, and assume a given solution, simplifying the solution of the circuit, these do not explain the asymmetrical behaviour of the first pulse in the laser voltage. The model proposed in this work allows to introduce all the elements of the laser circuit, or the analysis of more complex circuits, and the fire times of spark gap and the laser, producing a best fitting to the real operation of the circuit and to the experimental voltages. Finally the two steps model produce most suitable values for the inductances. A limitation of our model is that it does not consider the nonlinear properties of the spark gap and the laser.

REFERENCES

1. P. Persephonis, *J. Appl. Phys.* **62** (1987) 2651.
2. P. Persephonis, V. Giannetas, J. Parthenios, C. Georgiades and A. Ioannou, *IEEE, J. Quant. Electron.* **29** (1993) 2371.
3. T. Niewierowicz, L. Kawecki and J. de la Rosa, *Rev. Mex. Fís.* **41** (1995) 822.
4. P. Persephonis, V. Giannetas, C. Georgiades, J. Parthenios and A. Ioannou, *IEEE, J. Quant. Electron.* **31** (1995) 567.
5. P. Persephonis, V. Giannetas, C. Georgiades, J. Parthenios and A. Ioannous, *IEEE, J. Quant. Electron.* **31** (1995) 573.
6. A. Vázquez Martínez and V. Aboites, *IEEE, J. Quant. Electron.* **29** (1993) 2364.